

Discussions on multi-sensor Hidden Markov Model for human motion identification

NAN YU¹

Abstract. Based on acceleration sensor and gyroscope data fusion, a human motion identification method was put forward for tackling the problem of large error of monitoring human motion with single sensor. Measurement accuracy of attitude angle was greatly improved by revising attitude angle collected by acceleration sensor with human motion information outputted by gyroscope and achieving information fusion for multi-sensor using Kalman filtering algorithm. Hidden Markov Model (HMM) for identifying human motion was built based on characteristics of human attitude angle. Experiment showed that to identify physical exercise was more accurate with multi-sensor HMM based-method than with single sensor.

Key words. HMM, multi-sensor, human movement identification, data fusion.

1. Introduction

A human motion model for physical education was made up of head, the upper part of the body, the upper part of big arm, the middle and lower parts of big arm, forearm, hip, thigh, shank and feet. A new type of jointing element was used among those parts. This mode was used demonstrate various exercises for students or athletes to imitate and practice [1]. Therefore, recognition algorithm of HMM was adopted to analyze angular information and extract characteristics of several basic movements. Human movement mode was analyzed and identified in real time with the matching input sequence and HMM model.

2. Literature review

Two basic approaches for identifying movement were video image-based monitoring method and wearable device-based monitoring method. To collect and analyze depth image features, video inductor was introduced to video image-based monitor-

¹Tianjin University, Tianjin, 300072, China; E-mail: nprv5919@tom.com

ing method whose typical image processing method was based on kinect [2]. This method was featured limited monitored area, needing specific light for monitored area and unguaranteed privacy security for users. Mature technology-MEMS sensor was adopted by wearable device-based monitoring method, such as attitude detecting system made up of accelerometer, gyroscope and magnetometer were used to identify human motion information [3]. This method was featured guaranteed privacy security for users. This device was of low price and suitable for widely promotion.

Generally, acceleration sensor was used in motion detection technology because of its accurate identification in uniform variable speed [4]. However, most physical exercise was variable acceleration motion. Thus, there was large identification error because of gravitational acceleration and accelerated speed. Therefore, a wearable device was designed to collect data using acceleration sensor and gyroscope. More accurate and reliable identification information was obtained by fusing multi-source information with Kalman filtering. HMM recognition algorithm was used to analyze attitude angle and extract characteristic value of motor. Common human movement mode was analyzed and identified in real time by the matching input sequence and HMM model.

3. Research method

3.1. Data collection and fusion

A space coordinate system should be built before collecting human motion information. Performance of different body parts was very different during the same exercise because human motion was complex. Motion of the upper trunk (body parts above waist and under the neck) was relatively stable in daily activities while in walk, stand and fall down, its motion was evident. Thus, sensor was put on the upper trunk to collect data.

Human trunk coordinate system $oxyz$ (see figure 1) was built taking place of sensor as original point. Ground coordinate system was taken as fixed Cartesian coordinate system $OXYZ$. When human body stood still, human trunk coordinate system $oxyz$ was parallel to ground coordinate system $OXYZ$.

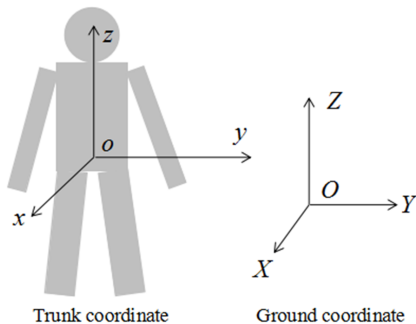


Fig. 1. Space coordinate system for human motion

3.2. Algorithm for information collection and fusion

Tri-axial digital acceleration sensor MMA7660 was used to collect human gravitational acceleration. MEMS tri-axial angular velocity sensor (gyroscope) L3G4200D was used to collect human attitude angle. Sampling frequency was set as 50Hz. The collected acceleration data and gyroscope data was transferred by information acquisition module to PC to fuse. Angular value collected by system was revised in real time by data that collected by acceleration sensor, thus deviation of attitude angle measurement caused by single sensor was addressed [5].

Given \mathbf{G} vector value measured by acceleration sensor when exercising. Acceleration magnitudes of \mathbf{G} in three coordinate axes X , Y and Z are G_x , G_y and G_z . Acceleration measurement should be converted to angular value and acceleration magnitude should be converted to angular value, which, in principle, is shown in Fig. 2.

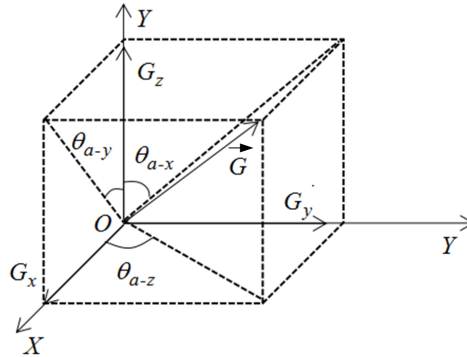


Fig. 2. Principle for measuring angular value with acceleration sensor

The given acceleration sensor was in idle state:

$$\mathbf{G}^2 = G_x^2 + G_y^2 + G_z^2 \quad (1)$$

First, normalize vector \mathbf{G} .

$$F_x = \frac{G_x}{|\mathbf{G}|}, F_y = \frac{G_y}{|\mathbf{G}|}, F_z = \frac{G_z}{|\mathbf{G}|} \quad (2)$$

The vector value \mathbf{F}_a in the direction of normalized gravity is computed using the formula

$$|\mathbf{F}_a| = \sqrt{F_x^2 + F_y^2 + F_z^2} = 1. \quad (3)$$

Included angles θ_{a-x} , θ_{a-y} and θ_{a-z} between the gravity vector and directions of three coordinate axes were calculated with normalized vector value. Method to

calculate the included angles was shown as follows:

$$\theta_{a-x} = \arcsin \left(\frac{|F_y|}{\sqrt{F_y^2 + F_z^2}} \right), \quad \theta_{a-y} = \arcsin \left(\frac{|F_x|}{\sqrt{F_x^2 + F_z^2}} \right),$$

$$\theta_{a-z} = \arcsin \left(\frac{|F_y|}{\sqrt{F_x^2 + F_y^2}} \right). \quad (4)$$

Given rotation angular speed measured by rotating angular velocity sensor around coordinate axes X , Y and Z of components ω_x , ω_y and ω_z . The measured angular velocity should be converted to corresponding rotation angle. According to the collected rotation angular velocity at present and system sampling period, rotation angle of gyroscope rotating around the direction of the three axes was calculated as

$$\theta_{gy-x} = \int \omega_x dt, \quad \theta_{gy-y} = \int \omega_y dt, \quad \theta_{gy-z} = \int \omega_z dt. \quad (5)$$

In the above formula, θ_{gy-x} , θ_{gy-y} and θ_{gy-z} denote corresponding rotation angles of axes X , Y and Z after calculation, respectively. Symbol dt denotes the sampling period of gyroscope data.

Kalman filter was used to fuse information collected by acceleration sensor and gyroscope. Regard acceleration sensor-measured value as predicted value and gyroscope-measured value as observed value. Predicted value revised by observed value was taken as the output value. Drift error b of the gyroscope estimated by the acceleration sensor was taken as the state vector, thus, the state equation and observation equation of system were shown as follows

$$\left\{ \begin{array}{l} \begin{bmatrix} \dot{\theta} \\ \dot{b} \end{bmatrix} = \begin{pmatrix} 0 & -1 \\ 0 & 0 \end{pmatrix} \begin{bmatrix} \theta \\ b \end{bmatrix} + \begin{bmatrix} 1 \\ 0 \end{bmatrix} \omega_{gy} + \begin{bmatrix} \omega_g \\ 0 \end{bmatrix} \\ \theta_a = [1 \quad 0] \begin{bmatrix} \dot{\omega} \\ b \end{bmatrix} + \omega_a \end{array} \right. \quad (6)$$

In formula (6), ω_{gy} denotes the angular velocity representing the output by gyroscope with fixed deviation. θ_a denotes the angular value of acceleration sensor after processing. Symbols ω_g and ω_a denote measurement noise of gyroscope and acceleration sensor. These two measurement noises are mutual independent. For the convenience of calculation, those two measurement noises are assumed to be normally distributed white noises. Given measurement noise of system $\omega(k)$ and sampling period is T_s . Thus, the state equation and measurement equation of system are as follows:

$$\begin{cases} X(k) = \begin{bmatrix} 1 & T_s \\ 0 & 1 \end{bmatrix} X(k-1) + \begin{bmatrix} T_s \\ 0 \end{bmatrix} \omega_{gy}(k-1) + \begin{bmatrix} \omega_g(k)T_s \\ 0 \end{bmatrix} \\ V_i = [1 \quad 0] X(k) + \omega_a(k) \end{cases}, \quad (7)$$

$$K_g(k) = \frac{P(k|k-1)H^T}{HP(k|k-1)H^T + \Gamma(k)}. \quad (8)$$

In formula (8), $K_g(k)$ denote the Kalman increment at time k . Symbol $P(k|k-1)$ denotes the covariance of system at time $k-1$. Symbol H denotes output matrix of measuring system and H^T denotes its transpose. $\Gamma(k)$ denotes the covariance of measurement noise. Thus, the fused attitude angle is given as follows:

$$\theta(k) = \theta_{gy}(k) + K_g(k)(\theta_{gy}(k) - \theta_a(k)). \quad (9)$$

In the above formula, $\theta_{gy}(k)$ and $\theta_a(k)$ denote the output attitude angle of gyroscope and acceleration sensor at time k , respectively. Symbol $\theta(k)$ denotes the output attitude angle after fusion at time k and the optimal value output by the Kalman filtering at time k . The covariance of the system state at time k was calculated using the formula

$$P(k|k) = (1 - K_g(k)H)P(k|k-1). \quad (10)$$

Formulae (6)–(10) represent the whole computing process of Kalman filtering. Formulae (8) and (10) were used to guarantee recursiveness and continuity of the filtering algorithm. When received output angular velocity of gyroscope at $k+1$ th time, the system would go back to formula (6). Thus, the system entered filtering algorithm at time $k+1$.

The collected multi-sensor data after fusion was more close to true value because measuring angle error of acceleration sensor was carried out. In order to explain effect of fusion algorithm, comparison charts of measurement attitude angle before and after fusion in X direction are shown in Figs. 3 and 4.

The attitude angle curve of stable walk is shown in Fig. 3. It can be seen from this figure that there is a small attitude angle change before and after data fusion. Those two curves were of high coincidence rate and data before fusion was of relatively small curve interference because measuring error of sensor was small when doing slow and stable exercise. Figure 4 shows attitude angle curve of fast walk, a strenuous exercise. It can be seen that the measured angles before and after data fusion were very different. When doing slow and stable exercise, angular value measured by sensor was of small interference and high accuracy. When doing strenuous exercise, the measured angular value was inaccurate because acceleration sensor was influenced by gravity and zero drift of gyroscope. Thus, multi-sensor data fusion was introduced to calculate the optimal estimated value in direction of motion vector, which method greatly lowered gravity vector displacement and zero drift those occurred because of interference of external force [6]. Therefore, smoothing and effective attitude angle

was obtained.

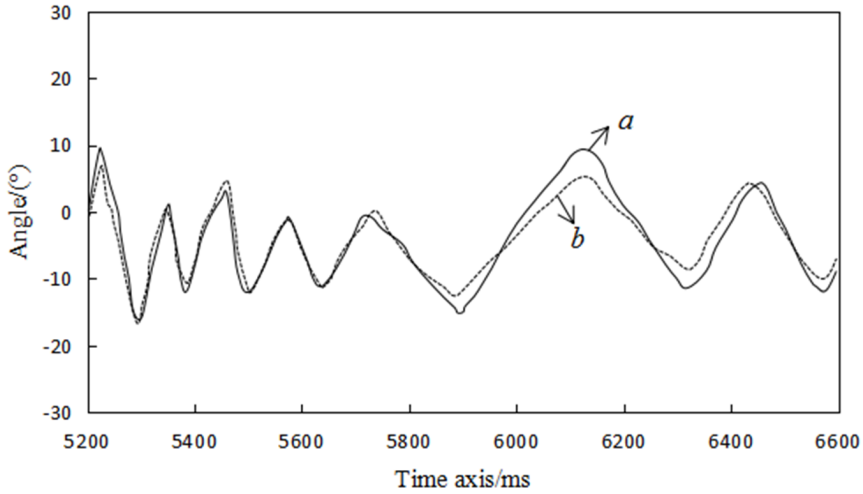


Fig. 3. Angle comparison of stable walk in X axis direction (a: before fusion, b: after fusion)

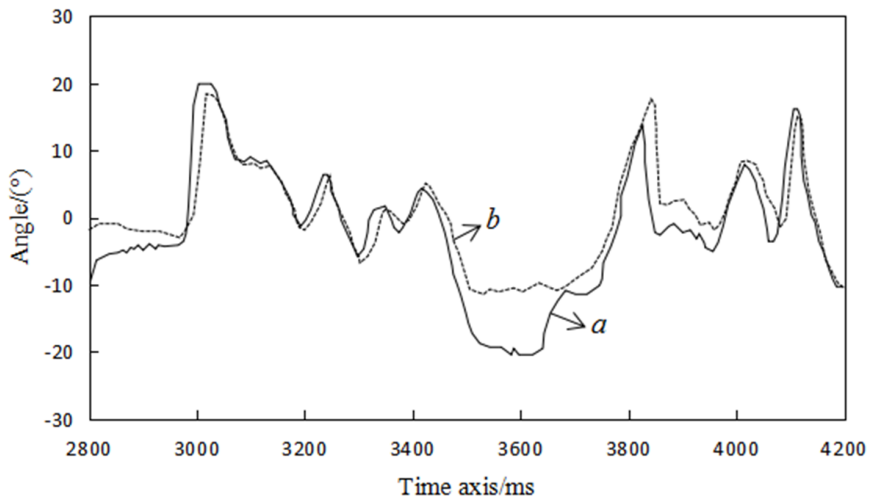


Fig. 4. Angle comparison of fast walk in X axis direction (a: before fusion, b: after fusion)

3.3. HMM model-based identification algorithm for specific motion

Markov chain is a Markov process with discrete parameters of time and state and a specific situation in Markov random process. Markov chain can be described as follows:

$$P(X_{m+k} = q_{m+k} / X_m = q_m, X_{m-1} = q_{m-1}, \dots, X_1 =$$

$$= q_1) = P(X_{m+k} = q_{m+k} / X_m = q_m), \quad (11)$$

where $q_1, q_2, \dots, q_m, q_{m+k} \in (\theta_1, \theta_2, \dots, \theta_N)$.

Matrix of transition probability is

$$A = \begin{bmatrix} a_{11} & \cdots & a_{1N} \\ \vdots & \ddots & \vdots \\ a_{N1} & \cdots & a_{NN} \end{bmatrix}$$

and

$$0 \leq a_{ij} \leq 1, \quad \sum_{a=1}^N a_{ij} = 1.$$

Several parameters below are used to describe a Hidden Markov Model (HMM):

A: $A = a_{ij}$ is the state probability transfer matrix. B: $B = b_j(k)$ is the probability matrix for the observed value. N : N is the state number of Markov chain in mode. Finally, π : $\pi = (\pi_1, \dots, \pi_N)$ is the state vector of the initial probability.

Given a HMM was $\lambda = (\pi, A, B)$. In other words, HMM was made up of two parts. One Markov chain was made up of π and A , producing output state sequence. Another one was a random process described by B , producing observed value sequence.

Standard Baum-Welch algorithm [7] was adopted to estimate HMM parameter. This algorithm was featured by a high timeliness while computation complexity was low. Updating weight with recursive computation effectively reduced its complexity, thus the model parameter that explained sample sequence more accurately was obtained. The computational process of this algorithm is shown below.

Defined variable $\delta_t(i, j)$ that corresponds to observed sequence O . Given S_i and S_j as the states at time t and time $t + 1$ respectively. Thus,

$$\begin{aligned} \delta_t(i, j) &= P(q_t = S_i, q_{t+1} = S_j | o_1, o_2, \dots, o_T) = \\ &= \frac{\alpha_t(i) a_{ij} b_j(o_{t+1}) \beta_{t+1}(j)}{\sum_i \sum_j \alpha_t(i) a_{ij} b_j(o_{t+1}) \beta_{t+1}(j)}. \end{aligned} \quad (12)$$

Defined variable $\eta_t(i)$. Given $\eta_t(i)$ denoted probability of observed sequence being in state S_i at time t . Thus,

$$\eta_t(i) = P(q_t = S_i | o_1, o_2, \dots, o_T) = \frac{\alpha_t(i) \beta_t(i)}{\sum_i \alpha_t(i) \beta_{t+1}(i)}. \quad (13)$$

It can be seen from formulae (12) and (13) that

$$a_{ij} = P(S | S) = \frac{\sum \delta_t(i, j)}{\sum \eta_t(i)},$$

$$b_j(k) = P(O|S) = \frac{\sum_{t,k} \eta_t(i)}{\sum \eta_t(i)}, \quad \pi_i = P(S) = \eta_t(i). \quad (14)$$

In this formula, a_{ij} , $b_j(k)$ and π_i are HMM parameters after reevaluation, thus new model was obtained.

Viterbi algorithm was based on dynamic programming. The optimal status switch was obtained with the observed output sequence. Mode was identified by Viterbi algorithm which was used to calculate likelihood. The computational process of Viterbi algorithm follows:

$$\sigma_t(i) = \max P(q_1 = S_i | o_1) = \pi_i b_i(o_1), \quad 1 \leq i \leq N, \quad (15)$$

$$W_i = 0. \quad (16)$$

Formula (16) represents the the initial condition for the system. After forward recursion, the below formula can be obtained

$$\begin{aligned} \sigma_t(j) &= \max P(q_1, q_2, \dots, q_t) = S_j, o_1, o_2, \dots, o_t), \\ &= \max[a_{ij} b_j(o_t) \max P(q_1, q_2, \dots, q_{t-1} = S_i, o_1, o_2, \dots, o_{t-1})], \\ &= \max[a_{ij} b_j(o_t) \sigma_t(i)], \quad 1 \leq i, j \leq N, \quad 2 \leq t \leq T. \end{aligned} \quad (17)$$

Formula (17) denotes the maximum value of $\sigma_t(j)$ at time t in state i . Given,

$$P = \max \sigma_t(j), \quad q_T = \arg \max[\sigma_t(i)]. \quad (18)$$

It was obtained with recursive operation $q_{t+1} \leftarrow q_t$, $t = 1, 2, \dots, T - 1$. The motion model corresponding to the maximum probability value is taken as identification result, which means that the state motion at present is identified. Flow chart for identifying human motion model is shown in Fig. 5.

4. Experiment and analysis

Based on characteristics of several basic movements, Weizmann data base and ten common movements in this data base including bend, jack, jump, pjump, run, side, skip, walk, wave1 and wave2 were compared to motion data obtained in experiment in order to compute identification rate. Model was built based on regarding those ten motion states as target object for identification. Ten athletes, ranging in age from 22 years old to 30 years old with normal height and weight and no limb illness, was chosen as monitoring objects. Two experiments (5 people in each experimental group) were done and its results was observed and compared. Single acceleration sensor was adopted by the first experimental group to collect human motion information for identifying motion mode. Multi-sensor data after fusion was used by the second experimental group to identify motion mode. Experimenters

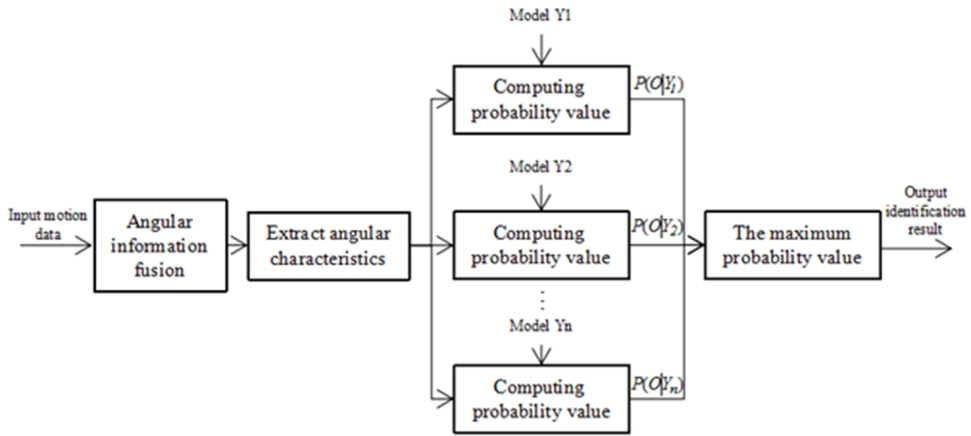


Fig. 5. Flow chart for identifying motion mode

should wear sensor across the upper limb and exercise randomly for one hour without external disturbance. Data collected by information collection module of sensor was transferred to upper computer through wireless communication module. Then, data was analyzed and motion mode was identified. Results of the experiment are shown in Table 1.

Table 1. Thermophysical properties of regular fluid and nanoparticles

State of motion	Identification rate of the first experimental group (%)	Identification rate of the second experimental group (%)
Bend	74.5	83.1
Jack	88.3	96.2
Jump	86.4	92.2
Pjump	81.3	88.4
Run	82.7	95.3
Side	75.3	82.7
Skip	86.9	91.1
Walk	83.5	92.3
Wave1	75.9	85.4
Wave2	79.1	89.7

It can be seen from Table 1 that the identification rate of the second experimental group was much higher than that of the first experimental group. Experiments verified that identifying human motion was more accurate with information fusion than with single sensor.

5. Conclusion

Acceleration sensor and gyroscope was adopted to collect changing information of attitude angle in different motion. Multi-sensor data was fused to extract characteristics of angular value. HMM motion mode was established to identify motion mode according to fusion characteristics. Experiment verified that identifying basic movements was more accurate with multi-sensor HMM based-method. Further study will be focused on classification and identification of relatively complex movements.

References

- [1] K. DAVIDS, C. BUTTON, D. ARAÚJO, I. RENSHAW, R. HRISTOVSKI: *Movement models from sports provide representative task constraints for studying adaptive behavior in human movement systems*. *Adaptive Behavior* 14 (2006), No. 1, 73–95.
- [2] E. C. NETO, E. S. REBOUCAS, J. L. DE MORAES, S. L. GOMES, P. P. REBOUCAS FILHO: *Development control parking access using techniques digital image processing and applied computational intelligence*. *IEEE Latin America Transactions* 13 (2015), No. 1, 272–276.
- [3] F. KHOSHNOUD, C. W. DE SILVA: *Recent advances in MEMS sensor technology – biomedical applications*. *IEEE Instrumentation & Measurement Magazine* 15 (2012), No. 1, 8–14.
- [4] F. SADI, R. KLUKAS: *Reliable jump detection for snow sports with low-cost MEMS inertial sensors*. *Sports Technology* 4 (2011), Nos. 1–2, 88–105.
- [5] A. KUBACKI, P. OWCZAREK, A. OWCZARKOWSKI, A. JAKUBOWSKI: *Construction and signal filtering in quadrotor*. *Progress in Automation, Robotics and Measuring Techniques*, book series AISC 351 (2015), 153–161.
- [6] B. MUNOZ-BARRON, J. R. RIVERA-GUILLEN, R. A. OSORNIO-RIOS, R. J. ROMERO-TRONCOSO: *Sensor fusion for joint kinematic estimation in serial robots using encoder, accelerometer and gyroscope*. *Journal of Intelligent & Robotic Systems* 78 (2015), No. 3, 529–540.
- [7] T. N. SAINATH, D. KANEVSKY, B. RAMABHADRAN: *Gradient steepness metrics using extended Baum-Welch transformations for universal pattern recognition tasks*. *IEEE International Conference on Acoustics, Speech and Signal Processing*, 31 March–4 April 2008, Las Vegas, NV, USA, *IEEE Conference Publications* (2008), 4533–4536.

Received May 7, 2017